



CRN/PN 91-18

**Statistical emission of complex fragments from
highly excited compound nucleus**

T. MATSUSE, S.M. LEE*, Y.H. PU*, K.Y. NAKAGAWA*, C. BECK
and T. NAKAGAWA*****

Faculty of Textile Science and Technology, Shinshu Univ., NAGANO 386, Japan

** Institute of Physics, Univ. of Tsukuba, IBARAKI 305, Japan*

*** Centre de Recherches Nucléaires, IN2P3-CNRS/Univ. Louis Pasteur,
67037 STRASBOURG CEDEX, France*

**** Cyclotron Laboratory, RIKEN, Wako, SAITAMA 351-01, Japan*

◆ ◆ ◆

*International Symposium NIKKO'91
Towards a Unified Picture of Nuclear Dynamics
NIKKO, Japan, June 6 - 8, 1991*

◆ ◆ ◆ ◆ ◆

**CENTRE DE RECHERCHES NUCLEAIRES
STRASBOURG**

IN2P3

CNRS

UNIVERSITE

LOUIS PASTEUR

920 1234

STATISTICAL EMISSION OF COMPLEX FRAGMENTS FROM HIGHLY EXCITED COMPOUND NUCLEUS

T. MATSUSE, S. M. LEE*, Y. H. PU*, K. Y. NAKAGAWA*
C. BECK** and T. NAKAGAWA***

Faculty of Textile Science and Technology, Shinshu Univ., NAGANO 386, Japan.

* Institute of Physics, Univ. of Tsukuba, IBARAKI 305, Japan.

** Centre de Recherches Nucléaires, et Université Louis Pasteur
B. P. 20, F-67037 Strasbourg, CEDEX, France.

*** Cyclotron Laboratory, RIKEN, Wako, SAITAMA 351-01, Japan

Abstract

In order to study the mechanism of complex fragments production from highly excited light and medium compound nucleus induced by relatively low energy heavy ion reactions, the full statistical analysis have been performed in terms of Extended Hauser Feshbach (EHF) method.

At first the charge- and kinetic energy- distributions of $^{35}\text{Cl} + ^{12}\text{C}$ reaction at ($E_{\text{Lab}} = 180,200$ MeV) and $^{23}\text{Na} + ^{24}\text{Mg}$ reaction at ($E_{\text{Lab}} = 89$ MeV) which form the ^{47}V compound nucleus of almost same excitation energy are extensively investigated as a prototype of the light mass system. The variations in observed cross section from fragment to fragment are understood by the variations of binding energy of the lighter fragments of binary decay from the compound nucleus. The difference of the yield in the measured cross sections between the reactions is interpreted as the entrance channel effect that $^{23}\text{Na} + ^{24}\text{Mg}$ channel has the larger critical angular momentum for fusion cross section than $^{35}\text{Cl} + ^{12}\text{C}$ channel. The measured kinetic energy distributions in the laboratory system of the complex fragments are shown to be well reproduced by the EHF-method. Therefore the observed complex fragment production are understood as the statistical binary decay from the compound nucleus induced by heavy-ion reaction.

Next, the EHF-method is extensively applied to the study of the complex production from the ^{111}In compound nucleus which formed by the $^{84}\text{Kr} + ^{27}\text{Al}$ reaction at ($E_{\text{Lab}} = 890$ MeV). Because the complex fragments (fissioning fragments) in the first step decay from this compound nucleus have large spins and highly excitation energies, the complex fragments decay sequentially by emitting the light particles. It is shown that the effect of multi-step cascade decay of fissioning fragments is very important for reproducing the general trend of the observed quantities such as the observed isotope-mass distributions.

1. Introduction

Although, the study on the mechanism of complex fragment production from hot nucleus may be one of the interesting subjects in the heavy ion physics in the intermediate energy region, it seems to be not straight forward to realize how to understand the reaction mechanism and what is important. Of course several models and physical pictures may exist for the studies, but it is even now very important to recognize that to what extend the full equilibrate model is valid for reproducing the observed quantities. Then we concentrate our investigation on the statistical emission of the complex fragments from highly excited compound nucleus formed in the relatively low energy heavy ion reactions.

Though it is better to study the phenomena comprehensively, in order to make

clear our aim, but we take the following two compound nuclei as the prototype in this study; ^{47}V compound nucleus of the lighter mass system and ^{111}In compound nucleus of the medium mass one. Because the general introduction of the aim of this study and reviews have been already presented by Heusch [1] and by Yuasa-Nakagawa [2], here some complementary introductions are given.

In the heavier mass system than $A_{CN} > 70$, it is well recognized that the fission-like phenomena really exist as the binary decay from the fused system in the low energy heavy-ion reactions such as $^{32}\text{S} + ^{78}\text{Ge}$ [3] and $^{32}\text{S} + ^{59}\text{Co}$ [4] reactions. Then it is expected to be measured the fission-like phenomena from the fused system in the lighter mass system $A_{CN} < 70$.

In recent years, Sanders et al. [5] have measured fully energy-dumped complex fragment production from the $^{32}\text{S} + ^{24}\text{Mg}$ reaction at ($E_{Lab} = 121,142$ MeV) and concluded that the fragments can be understood as the binary decay (fission-like decay) from the compound nucleus. They have also discussed the reaction mechanism in terms of the transition-state model [6] and the equilibrium orbiting-model [7] and showed that the transition-state model reproduces well the general trend of the mass distributions. But it seems to be noticed that they have needed the introduction of the Wigner term to the mass of the decaying fragments with α -like nuclei in order to get the enhancements in the mass distribution.

In the more lighter mass system, the complex fragment's detection has been performed by means of a kinematical coincidence technique in the $^{35}\text{Cl} + ^{12}\text{C}$ reaction at a bombarding energies of 180 MeV [8], and 200 MeV [9] and the charge distributions have been obtained with the large fluctuations from fragment to fragment. It is also discussed [9] that the origin of the heavy fragment production is the fusion-fission of the ^{47}V compound nucleus rather than an orbiting mechanism.

Before the performance of these essential experiments [5,8,9] on the measurements of fission-like fragments, we have already proposed to extend the Hauser-Feshbach method (EHF-method) to the calculation of the cross section of decaying complex fragments (fission-like fragments) from the fused system induced by the heavy ion reaction [10]. The EHF method should be considered to attempt for treating light-particle emission and complex fragment production (fission-like production) in the equivalent statistical way from a view point of scission point model. Especially if we adequately use the observed binding energy of the fragments in the phase space calculation, it has shown that EHF-method is very valid for reproducing the fission-like cross sections of the medium mass systems [11]. Then the EHF-method have been applied to the interpretation of the fission-like phenomena of the reactions $^{32}\text{S} + ^{24}\text{Mg}$ at ($E_{Lab} = 121,142$ MeV) and $^{35}\text{Cl} + ^{12}\text{C}$ at ($E_{Lab} = 180,200$ MeV) and we have showed that the observed complex fragment production are understood as the statistical binary decay from the compound nucleus induced by heavy-ion reaction [13]. A brief presentation is given on the EHF-method for these lighter mass system in section 2.

More recently Djerroud et al [13] have performed the experiment of $^{23}\text{Na} + ^{24}\text{Mg}$ reaction at ($E_{Lab} = 89$ MeV) which forms the ^{47}V compound nucleus of almost same excitation energy with that of the $^{35}\text{Cl} + ^{12}\text{C}$ reactions [8],[9]. The important point of these experiments is that these two channels with different mass asymmetry forms the ^{47}V nucleus with the same excitation energy ($E_{CN}^* = 64$ MeV) and the full equilibrated cross sections (fusion-fission-like and fusion-evaporation) have been completely measured in the both channels. It is obtained that the fission-like fragments of the $^{23}\text{Na} + ^{24}\text{Mg}$ reaction have the larger cross sections than that of the $^{35}\text{Cl} + ^{12}\text{C}$ reaction but the measured charge distributions in the both channels show the almost same fluctuation from fragment to fragment. The discussion on the difference in the observed

quantities between the $^{35}\text{Cl} + ^{12}\text{C}$ reaction at $E_{\text{Lab}} = 200\text{MeV}$ [9] and $^{23}\text{Na} + ^{24}\text{Mg}$ reaction at $E_{\text{Lab}} = 89\text{MeV}$ [13] is presented by showing the calculated results of EHF-method in Section 3.

On the complex fragment production from the ^{111}In compound nucleus, we concentrate how the EHF-method can reproduce the observed quantities which measured in the reaction of $^{84}\text{Kr} + ^{27}\text{Al}$ at $E_{\text{Lab}} = 890\text{MeV}$ [2]. The preliminary results and discussion on this reaction have already been presented [14]. As can be seen the measured charge distribution (see Fig.4 of Ref[2]), not only the fission-like fragments have the large cross section and but also the significant enhancements have been measured in the mass region of intermediate fragments $Z < 10$. Then it is interesting that the obtained critical angular momentum J_{cr} for the total fusion cross section formation exceeds the limit of the Rotating Liquid Model (see the discussion in Ref.[2]). Furthermore the essential point of the experiment is that the isotope mass distributions for all complex fragment production have been measured (see Fig.11 of Ref[2]). These observed isotope mass distributions will give a good criterion for identifying the full equilibrated nature of the ^{111}In compound nucleus.

Because the formed compound nucleus ^{111}In of this experiment has the high excitation energy $E^* = 216\text{MeV}$, it is easily expected that the emitted complex fragments and evaporation residues at the first step emission have the highly excited energy and spin distributions and the multi-step cascade decays occur sequentially. In this report the effect of the multi-step cascade calculation are discussed by showing the calculated results of the charge, isotope-mass and kinetic energy distributions in section 4.

The detailed interpretations on the interrelation of this experiment and the other ones such as $^{84}\text{Kr} + ^{27}\text{Al}$ at $E_{\text{Lab}} = 5.8$ and 35MeV/u and $^3\text{He} + \text{Ag}$ at $E_{\text{Lab}} = 30$ and 65MeV/u are shown by Yuasa-Nakagawa [2].

2. Extended Hauser-Feshbach Method

The outline of Extended Hauser-Feshbach method is shown to calculate the cross sections of the full statistical binary decay from the highly excited compound nucleus. Incident channel with projectile (Z_P, A_P) and target (Z_T, A_T) of CM-energy E_{CM} forms the compound system ($Z_{\text{CN}}, A_{\text{CN}}$) of excitation energy E^* . Here, $E^* = E_{\text{CM}} + Q_0$, and Q_0 is Q-value of incident channel. The total angular momentum is represented by J . The formed compound state decays through the usual particle evaporation of n, p, α and the binary decay of complex fragment set ((Z_L, A_L) and (Z_H, A_H)) with angular momentum L and energy E of the relative motion and channel spin I .

Because we consider only full statistical decay from the compound nucleus, it is assumed that the averaged S -matrix $|S_{L,I}^{(J)}(E)|^2$ is available for calculating the cross section. And the cross section of an exit channel is represented by the usual formula in the case of initial channel spin zero.

$$\frac{d^2\sigma}{d\Omega dE} = \frac{\pi\hbar^2}{2\mu_c E_{\text{CM}}} \sum_J (2J+1) \sum_{L,I} |S_{L,I}^{(J)}(E)|^2 \sum_M (I - M L M |J 0\rangle^2 |Y_{LM}(\theta\phi)|^2 \quad (1)$$

Here μ_c denotes the reduced mass of the incident channel.

Extended Hauser-Feshbach method

In order to calculate the averaged S -matrix, the Hauser-Feshbach method is applied. By the use of the phase space $N_{L,I}^{(J)}(E)$ of a exit channel, the averaged S -matrix is defined

by the following formula

$$\overline{|S_{L,I}^{(J)}(E)|^2} = T_{(J)}^{(fus)}(E_{CM}) \frac{N_{L,I}^{(J)}(E)}{D^{(J)}} \quad (2)$$

Here $T_{(J)}^{(fus)}(E_{CM})$ is the transmission coefficient of the initial channel which forms fusion cross section. In this study we use following simple distribution for the transmission coefficient,

$$T_{(J)}^{(fus)}(E_{CM}) = \frac{1}{1 + \exp((J - J_{cr})/\Delta_J)} \quad (3)$$

The critical angular momentum J_{cr} is determined by our fusion model (see reference [15] for details). The defuseness parameter Δ_J is used to be $1\hbar$ in the present calculation. The total phase space $D^{(J)}$ is represented by the following formula as the summation of whole decay channels f

$$D^{(J)} = \sum_f \int \sum_{(L,I)J} N_{L,I}^{(J)}(E) dE + N_{\gamma}^{(J)}(E^*) \quad (4)$$

Here $N_{\gamma}^{(J)}(E^*)$ denotes the phase space of γ -ray decay. In our calculation giant-E1-transition is included.

Phase space of light particle evaporation

The usual Hauser-Feshbach Method is used to calculate the phase space of the light particle evaporation and the formula is represented as follows

$$N_{L,I}^{(J)}(E) = \int \rho_I(\epsilon) T_L(E) \delta(\epsilon + E + Q - E^*) d\epsilon \quad (5)$$

Here $T_L(E)$ is the transmission coefficient of the n, p, α channel and are calculated by the use of the standard optical potential model. Level density formula $\rho_I(\epsilon)$ which has been shown by Bohr and Mottelson [16] is used

$$\rho_I(\epsilon) = \frac{1}{24} \left(\frac{a\hbar^2}{2g} \right)^{3/2} (2I + 1) a \frac{e^{2\sqrt{X}}}{X^2} \quad (6)$$

Here X is defined by the following formula

$$X = a \left(\epsilon - \frac{\hbar^2}{2g} I(I + 1) - \Delta_{pair} \right) \quad (7)$$

ϵ is the whole excitation energy of the residual nucleus.

In this calculation the shell structure effect of the nucleus is introduced to the level density parameter a as the temperature dependent one (see the details Ref[12]). Moment of inertia g is evaluated by the following rigid body one. $g = \frac{2}{5} AM_n (r_0 A^{1/3})^2$ where $r_0 = 1.2\text{fm}$ is used here and M_n is the nucleon mass. The pairing energy $\Delta_{pair} = \Delta_n + \Delta_p$ is evaluated by the use of the formula which is given in Ref.[16], The value of Q is the usual separation energy which is evaluated by the following formula,

$$Q = B_{GS}(N_{CN}, Z_{CN}) - B_{GS}(N_L, Z_L) - B_{GS}(N_H, Z_H) \quad (8)$$

where the $B_{GS}(N, Z)$ is the observed binding energy of Ref.[17]. Then it should be noticed that the calculated phase space depends strongly on the binding energy of the decaying fragments.

Phase-space of the complex fragment and fission

To calculate the phase space of the complex fragment, we categorize into two parts. The first one is the discrete low excitation below the threshold of the light particle's separation energy. The second one is the usual statistical excitation which is represented by the level density formula of eq.(6). Then the calculation of the phase space of the complex fragment and fission is divided into four parts as follows.

$$N_{LI}^{(J)}(E) = N_{LI}^{(J)}(E)^{(1)} + N_{LI}^{(J)}(E)^{(2)} + N_{LI}^{(J)}(E)^{(3)} + N_{LI}^{(J)}(E)^{(4)} \quad (9)$$

$$N_{LI}^{(J)}(E)^{(1)} = \int \int \sum_{(I_L, I_H)I} \rho_{I_L}(\epsilon_L) \rho_{I_H}(\epsilon_H) T_L(E) \delta(\epsilon_L + \epsilon_H + E + Q - E^*) d\epsilon_L d\epsilon_H \quad (10)$$

$$N_{LI}^{(J)}(E)^{(2)} = \sum_i \int \sum_{(I_L, I_H)I} \rho_{I_H}(\epsilon_H) T_L(E) \delta(\epsilon_{L_i} + \epsilon_H + E + Q - E^*) d\epsilon_H \quad (11)$$

$$N_{LI}^{(J)}(E)^{(3)} = \sum_j \int \sum_{(I_L, I_H)I} \rho_{I_L}(\epsilon_L) T_L(E) \delta(\epsilon_L + \epsilon_{H_j} + E + Q - E^*) d\epsilon_L \quad (12)$$

$$N_{LI}^{(J)}(E)^{(4)} = \sum_i \sum_j \sum_{(I_L, I_H)I} T_L(E) \delta(\epsilon_{L_i} + \epsilon_{H_j} + E + Q - E^*) \quad (13)$$

Here the discrete levels are represented by the use of i and j for lighter part and heavier part of binary fragment, respectively. The i -th discrete excitation energy and spin of lighter part is represented by $(\epsilon_{L_i}, I_{L_i})$. The j -th discrete excitation energy and spin of heavier one is represented by $(\epsilon_{H_j}, I_{H_j})$.

Evaluation of the transmission coefficient $T_L(E)$

The transmission coefficient $T_L(E)$ at the scission point of the relative motion between two fragments is simply represented by the following formula for all type of the excitation of the fragments

$$T_L(E) = \frac{1}{1 + \exp((V(L) - E)/\Delta_L)} \quad (14)$$

where Δ_L is the defuseness parameter and the value of 1MeV is used for all channels. In this calculation we use the Krappe-Nix potential [18] for evaluating the barrier height of $V(0)$. This $V(0)$ is the Coulomb barrier V_c of the relative motion between binary fragments. Then the barrier height $V(L)$ in the relative motion for angular momentum L is parameterized by the use of the following simple formula ,

$$V(L) = V(0) + \frac{\hbar^2}{2\mu_f R_s^2} L(L+1) \quad (15)$$

where μ_f is the reduced mass between fragments. Here R_s is the scission point between fragments.

Here, in order to make clear the physical picture of our model, we introduce the barrier height of the scission point V_s for total spin $J = 0$ and angular momentum $L = 0$ which is measured from the ground state of the compound nucleus as follows,

$$V_s = V_c + Q. \quad (16)$$

The schematic representation is given in the Fig.2(b). As can be understood from the formulae of phase space calculation which are shown in the above equations, the values of the phase space are essentially limited by this barrier height of V_s for the case of total spin $J = 0$.

3. Results and discussions for ^{47}V compound nucleus

The calculated charge distributions of $^{35}\text{Cl} + ^{12}\text{C}$ and $^{23}\text{Na} + ^{24}\text{Mg}$ reactions are shown in Fig.1 by comparing with the experimental ones in the wide charge range from fusion-fission-like to fusion-evaporation distributions [8,9,13]. On the charge and kinetic energy distributions of $^{35}\text{Cl} + ^{12}\text{C}$ at $E_{Lab} = 180\text{MeV}$ shown in Fig.1(a), we have already discussed in Ref.[12]. One of the main aim of this report is to discuss the difference in the observed quantities between the $^{35}\text{Cl} + ^{12}\text{C}$ reaction at $E_{Lab} = 200\text{MeV}$ [9] and $^{23}\text{Na} + ^{24}\text{Mg}$ reaction at $E_{Lab} = 89\text{MeV}$ [13] by comparing with the calculated results of EHF-method.

The important point is that these two channels with different mass asymmetry forms the ^{47}V nucleus with the same excitation energy ($E_{CN}^* = 64\text{MeV}$) and the full equilibrated cross sections σ_{fus} (fusion-fission-like σ_{FF} and fusion-evaporation σ_{FE}) have been completely measured in the both channels. The values of the J_{cr} for the total fusion cross section formation (see eq.(3)) are obtained by the use of the measured fusion cross sections σ_{fus} as follows; the $J_{cr} \simeq 24\hbar$ for the $^{35}\text{Cl} + ^{12}\text{C}$ reaction at $E_{Lab} = 200\text{MeV}$ [9] and $J_{cr} \simeq 29\hbar$ for the $^{23}\text{Na} + ^{24}\text{Mg}$ reaction at $E_{Lab} = 89\text{MeV}$ [13]. Then it is expected that the larger fusion fission-like cross sections in the $^{23}\text{Na} + ^{24}\text{Mg}$ reaction than in $^{35}\text{Cl} + ^{12}\text{C}$ reaction is reasonably understood by the difference of the observed J_{cr} -values.

It is very interesting that these obtained J_{cr} -values are well reproduced by our fusion model [15]. In the case of entrance channel with mass symmetric $^{23}\text{Na} + ^{24}\text{Mg}$ at $E_{Lab} = 89\text{MeV}$, the fusion cross section is limited by the statistical yrast line, on the other hand the fusion cross section with asymmetric mass entrance channel of $^{35}\text{Cl} + ^{12}\text{C}$ at $E_{Lab} = 200\text{MeV}$ is determined by the successive critical distance [15]. Then we can discuss what is the entrance channel effect.

As can be seen in Fig.1, the over all of the observed charge distributions are well reproduced by the EHF-method calculation. The charge distributions with $Z < 11$ which correspond to the fusion fission-like one are the first-step binary decay from the ^{47}V compound nucleus. On the other hand the charge distributions with $Z > 12$ which correspond to the fusion evaporation are the result of multi-step cascade calculation. The reason why the EHF-calculation for these reactions can well reproduce not only the yields of the measured cross sections but also the variations from fragment to fragment is that the observed binding energy for the binary fragments at scission point is used to evaluate the separation energy Q -value (see eq.(8)). In Fig.2(a) it is shown how the barrier height of the scission point depends on the Q -values of the decaying fragments. The schematic interpretation of relation between the barrier height of scission point V_s defined in eq.(16) and the Coulomb barrier V_c in the relative motion is shown in Fig.2(b). Because so-called α -like nuclei in the p-shell and sd-shell region have strong binding energy, barrier height V_s of the α -like fragments becomes low. Then the strong

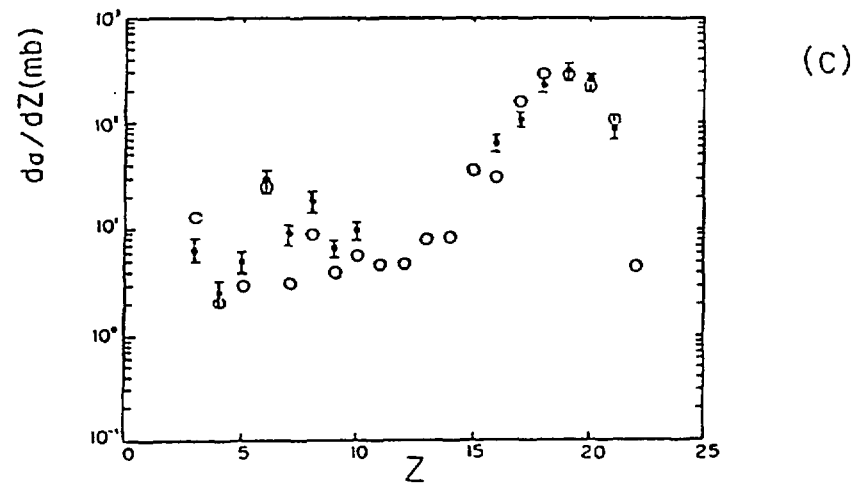
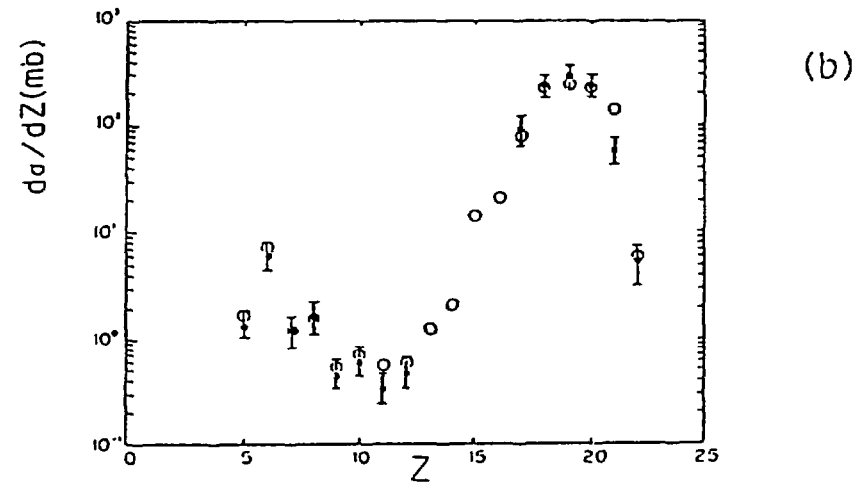
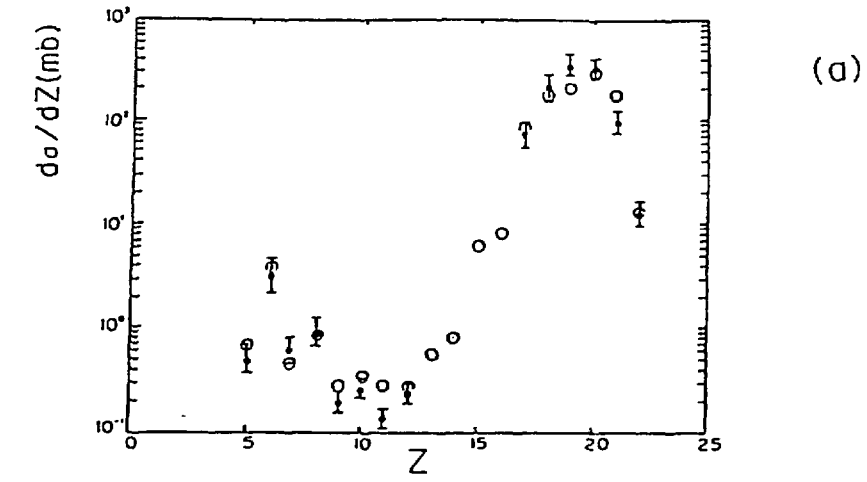


Fig.1 Comparisons of calculated charge distributions (open circles) by EHF-method with experimental ones (solid circles). (a) $^{35}\text{Cl} + ^{12}\text{C}$ reaction at $E_{\text{Lab}} = 180\text{MeV}$ [8], (b) $^{35}\text{Cl} + ^{12}\text{C}$ reaction at $E_{\text{Lab}} = 200\text{MeV}$ [9], (c) $^{23}\text{Na} + ^{24}\text{Mg}$ reaction at $E_{\text{Lab}} = 89\text{MeV}$ [13].

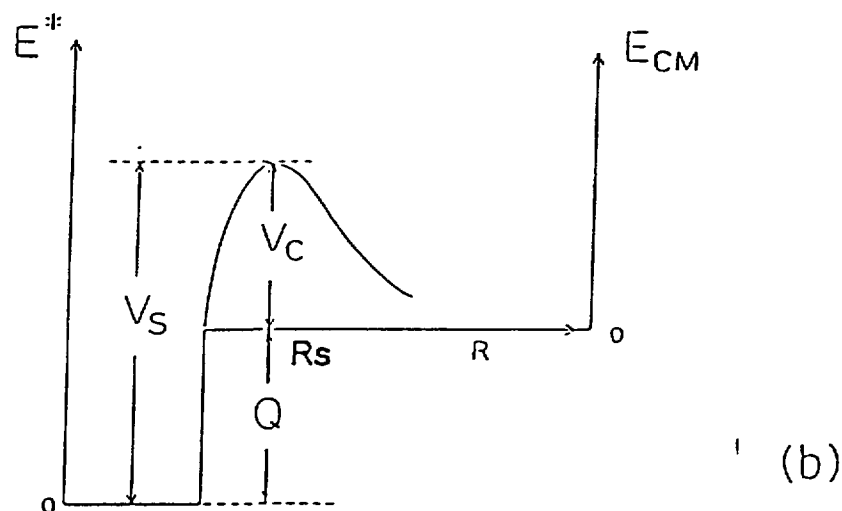
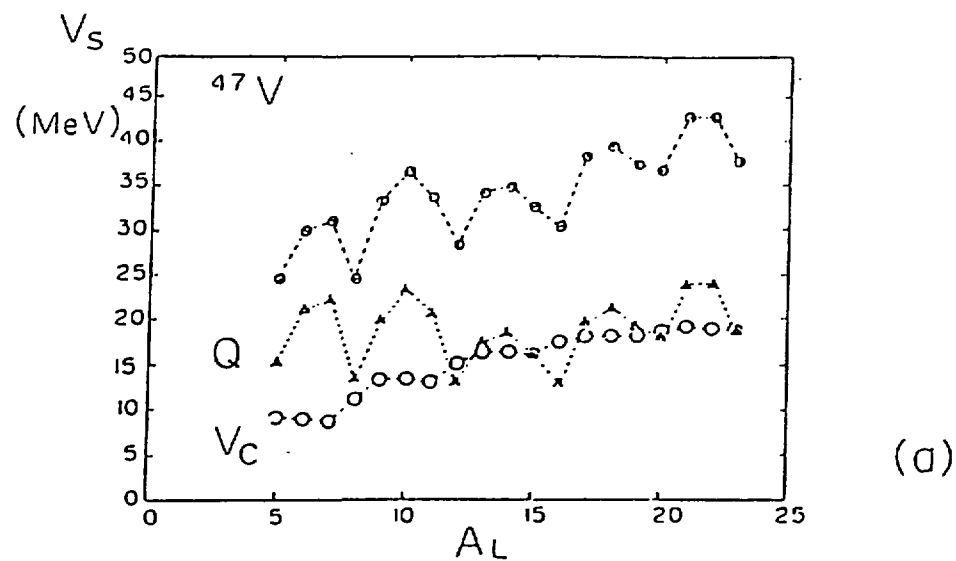


Fig.2 (a) Fission fragments dependence of barrier height of scission point for the ^{47}V -compound nucleus. Variable A_L shows the mass number of the lighter part of binary decay from compound nucleus. The plotted barrier height V_s (closed circles) of scission point are the lowest barrier in the available binary configurations for total spin $J = 0$ and angular momentum $L = 0$. Open circles and triangles show the Coulomb barriers V_c and Q -values, respectively. (b) The schematic representation of relation between barrier height V_s of scission point and Coulomb barrier V_c . The V_s is measured from the ground state of the compound system and V_c is defined by the relative distance R between decaying binary fragments. The R_s is the distance of scission point. The Q denotes the separation energy of the decaying binary fragment from the compound nucleus.

enhancement with even Z in charge distributions is reasonably understood. Therefore the nascent fragment from the compound nucleus around the scission point are expected to have the almost same properties of the individual nucleus.

In order to show how the fusion fission-like cross section depends to the total spin J -values, the partial wave dependence of the competition between fission-like and evaporation cross section obtained by EHF-calculation are shown in Fig.3 and 4. In this calculation the cross sections with $4 < Z < 11$ are considered as the fission-like cross section. From these calculated results the onset partial wave of the fission-like fragments production is expected to be about $20\hbar$. In these energy region the ratio of the fission-like cross section is very small by comparing the total fusion cross section, but the competition between fusion-like and evaporation occurs in somewhat smoothly with wide width in spin space as can be seen in the inset of Fig.3. As concern with the reactions $^{35}\text{Cl} + ^{12}\text{C}$ at $E_{\text{Lab}} = 200\text{MeV}$ and $^{23}\text{Na} + ^{24}\text{Mg}$ at $E_{\text{Lab}} = 89\text{MeV}$,

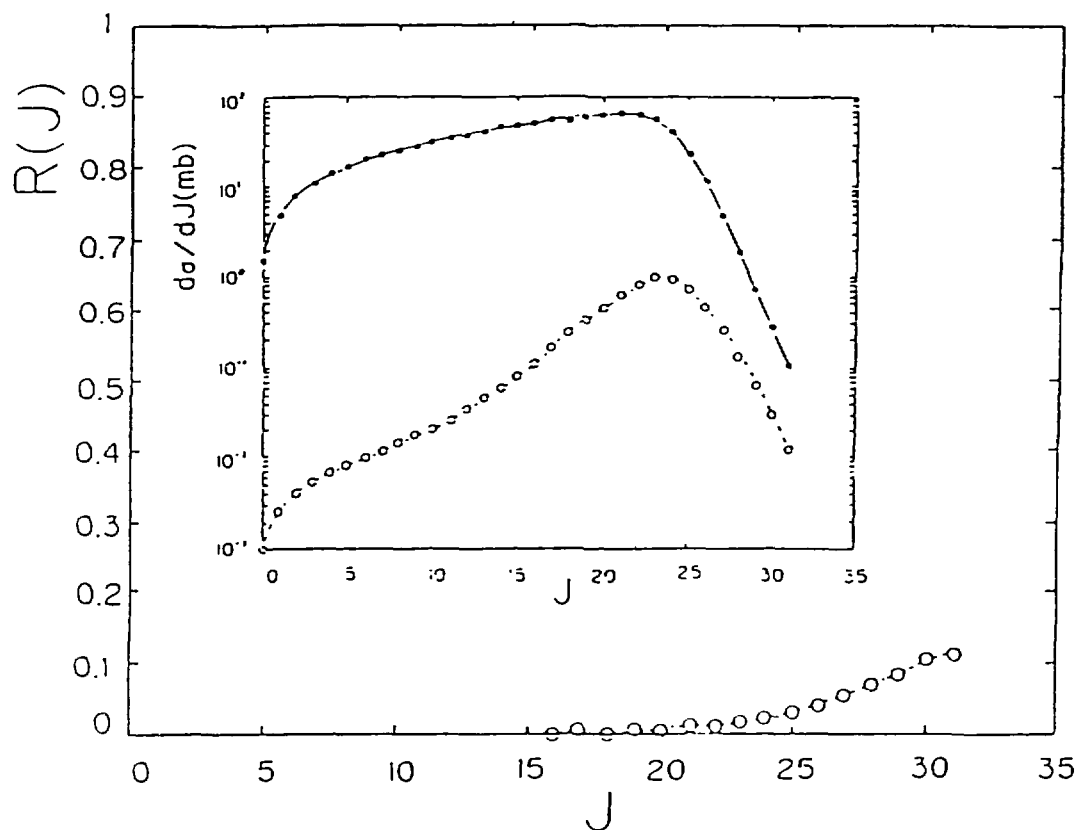


Fig.3 Partial wave dependence of competition between fission and evaporation cross sections obtained by EHF-method calculation for the $^{35}\text{Cl} + ^{12}\text{C}$ reaction at $E_{\text{Lab}} = 180\text{MeV}$. The inset are the partial wave dependence of evaporation cross section (closed circles) and fission one (open circles). The solid line shows the total fusion cross section.

because the J_{cr} -values for the total fusion cross sections are different in the two

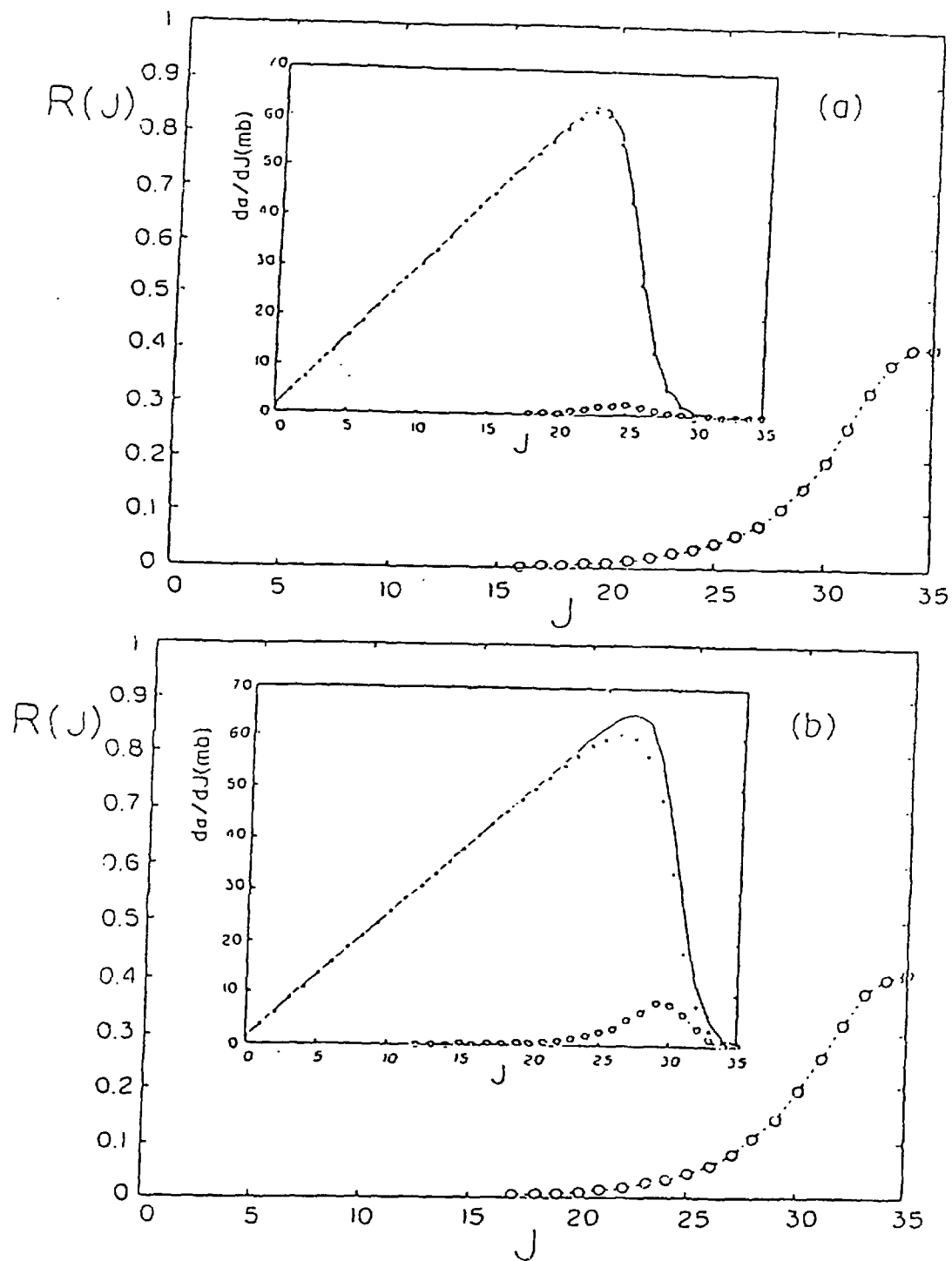


Fig.4 Partial wave dependence of competition between fission and evaporation cross sections obtained by EHF-method calculation. (a) $^{35}\text{Cl} + ^{12}\text{C}$ reaction at $E_{\text{Lab}} = 200\text{ MeV}$. (b) $^{23}\text{Na} + ^{24}\text{Mg}$ reaction at $E_{\text{Lab}} = 89\text{ MeV}$. The inset are the partial wave dependence of evaporation cross section (closed circles) and fission one (open circles). The solid line shows the total fusion cross section.

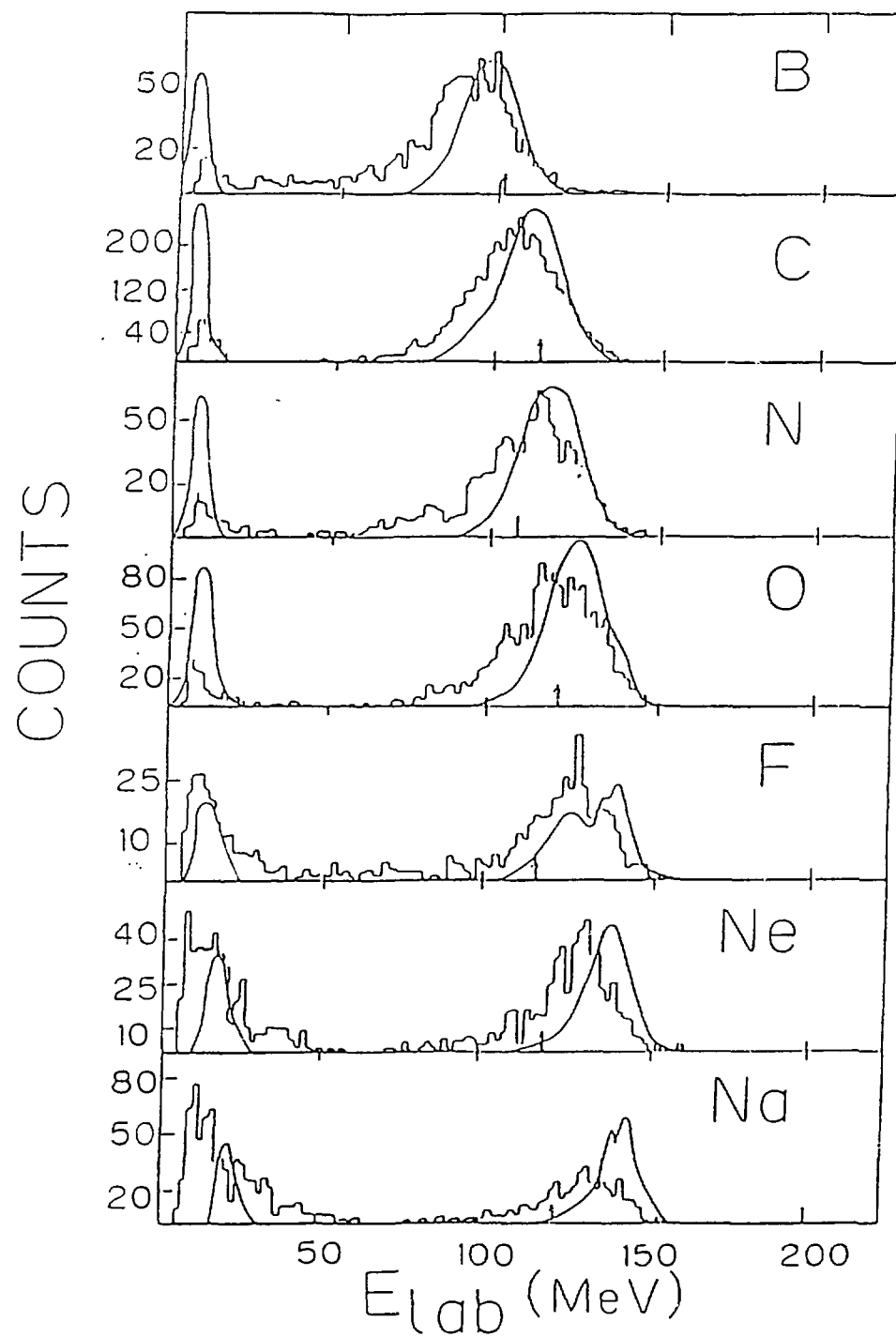


Fig.5 Comparisons of calculated kinetic energy distributions of fission fragments in the Lab-system by EIF-method (solid line) with the observed cases of $^{35}\text{Cl} + ^{12}\text{C}$ reaction at $E_{\text{Lab}} = 200\text{MeV}$ (histograms) at $\theta_{\text{Lab}} = 12^\circ$.

channels as mentioned above, the $^{23}\text{Na} + ^{24}\text{Mg}$ channel has larger fission-like cross section than $^{35}\text{Cl} + ^{12}\text{C}$ channel (see the insets of Fig.4), but the calculated partial wave dependence of the competition between fission-like and evaporation are completely same with both channels.

In Fig.5, the calculated kinetic energy distributions for the case of $^{35}\text{Cl} + ^{12}\text{C}$ reaction at $E_{\text{Lab}} = 200\text{MeV}$ are shown for the lighter fission-like fragments. The calculated kinetic energy distributions in the CM-system are transformed to the laboratory system by assuming that the angular distribution of decaying fragment in the CM-system has the $1/\sin(\theta)$ dependence. By comparing with the calculated and the measured kinetic energy distributions, the calculated results reproduce well the observed ones. Then we can conclude that the observed fission-like fragments are the statistical binary decay from the compound nucleus.

4. Results and discussions for ^{111}In compound nucleus

Because the general introduction and aim of this study on the reaction $^{84}\text{Kr} + ^{27}\text{Al}$ at $E_{\text{Lab}} = 890\text{MeV}$ have been already presented by Heusch [1] and by Yuasa-Nakagawa [2] including the essential parts of the calculated results by EHF-method at this conference, here some complementary interpretations are shown on the calculated results.

From the measured charge distribution and the evaporation cross section (see Fig.4 of Ref.[2]), the critical angular momentum are deduced to be $J_{\text{cr}} \simeq 83\hbar$ for the formation of the total fusion cross section. It is very interesting experimental result that this obtained J_{cr} exceeds the limit of the Rotating Liquid Model, but our fusion model predicts the almost same value of the experimentally obtained one (see Fig.5 of Ref.[2]). Then we use the critical angular momentum $J_{\text{cr}} = 83\hbar$ for the total fusion cross section in this calculation of EHF-method. The used parameters in this calculation are the almost same that of the case of the lighter mass system such as ^{47}V compound nucleus, but the static quadrupole deformation is introduced to the binary fragments at scission point with the collinear configuration in the case that the fragments excite statistically.

On the first step EHF-calculation.

Before showing the results of the multi-step cascade calculation, at first the calculated results of the first step are shown. The competition between fission-like and evaporation production how depend to the partial wave is shown in Fig.6. In this calculation the cross sections with $Z > 5$ are included in the fission-like production. The calculated cross section of evaporation residues is about 500mb in the first-step calculation and the onset partial wave for fission-like production is about $50\hbar$. Then in the partial wave region $J > 60\hbar$ the fission-like production becomes dominant than the light particle productions.

Because the formed compound nucleus ^{111}In has the high excitation energy $E^* = 216\text{MeV}$ in this experiment, it is easily expected that the residue nuclei of particle emission and fission-like fragments has the highly excited energy distribution at the first-step decay from the compound nucleus. In Fig.7(a) the calculated excitation energy distribution is shown for the residue nuclei of neutron and it can be understood that the residue nuclei have highly excited energy distribution. In the insets of the Fig.7(a) the calculated spin distribution is presented. As can be expected from the Fig.6, the spin distribution of the residue nuclei are almost same that of the spin distribution of the evaporation production because the relative motion between light particle and residue nuclei can not take out the large angular momentum. Then multi-step cascade decays from highly excited residue nuclei occur sequentially. Because the spin distributions of

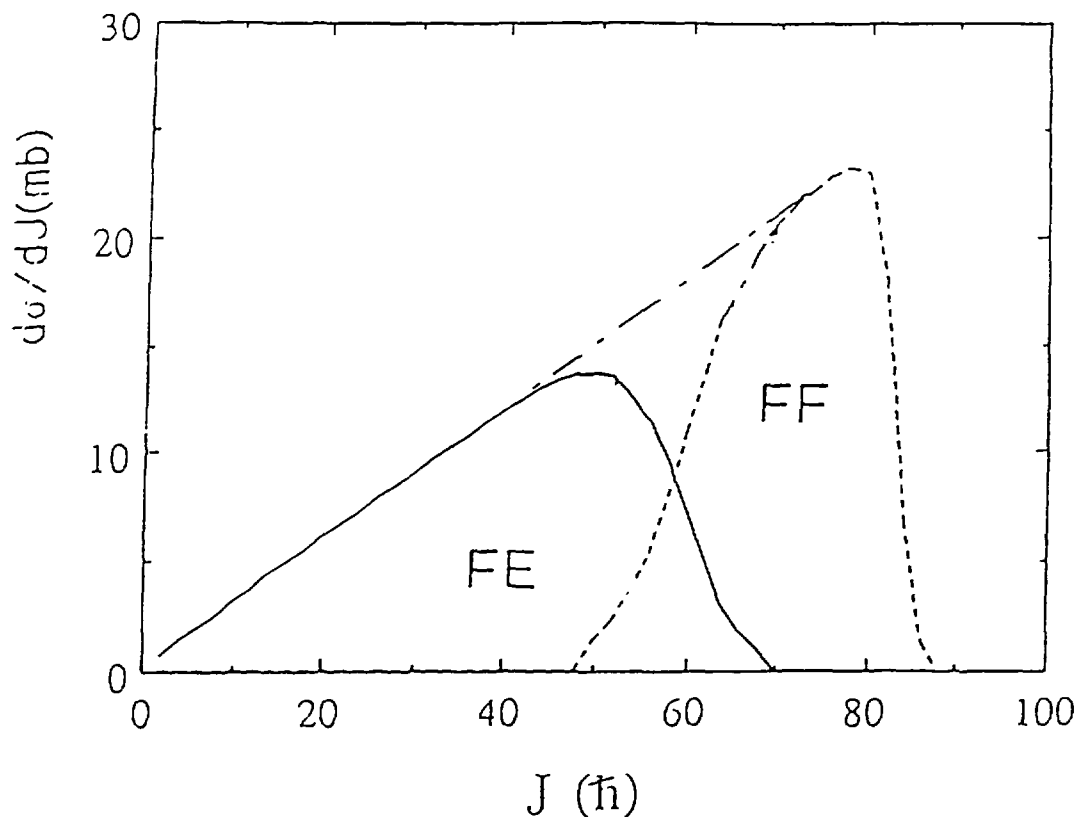


Fig.6 Partial wave dependence of fission (dashed line) and evaporation cross section (solid line) obtained by EHF-method calculation for the $^{84}\text{Kr} + ^{27}\text{Al}$ reaction at $E_{\text{Lab}} = 890\text{MeV}$. Total fusion cross section is shown by half-dashed line with $J_{\text{cr}} = 83\hbar$.

the residue nuclei have high spin one but not so high for fission-like production as can be expected from Fig.6, it is expected to be possible that the complex fragments with light mass such as $Z < 10$ may be produced in the process step of the multi-step cascade which start from the first step residue nuclei. In fact a large part of the enhancement of the light fragment cross section from the first step one to final step are accumulated through this multi-step cascade decay as shown in Fig.8.

On the other hand the fission-like fragments with heavier mass such as $Z < 30$ have the excitation energy and spin distributions as shown in Fig.7(b). The reason why the spin values of the fission-like fragments are not so large is that the relative motion between the fission-like fragments take out the large angular momentum. The energy distribution are well determined by the barrier height of scission point and the equipartition of energy between the two fragments. The obtained spin and energy distributions of the fission-like fragments are almost similar to the partial wave distribution and energy of the ^{47}V nucleus as presented above (see Fig.3 and 4). Then these fission-like fragments also decay by emitting the light particles, but the light fragments production is not important in these cascade decay. Of course because the produced light fragments such as $Z \simeq 10$ at the first step excite to somewhat high spin around $J \simeq 10\hbar$

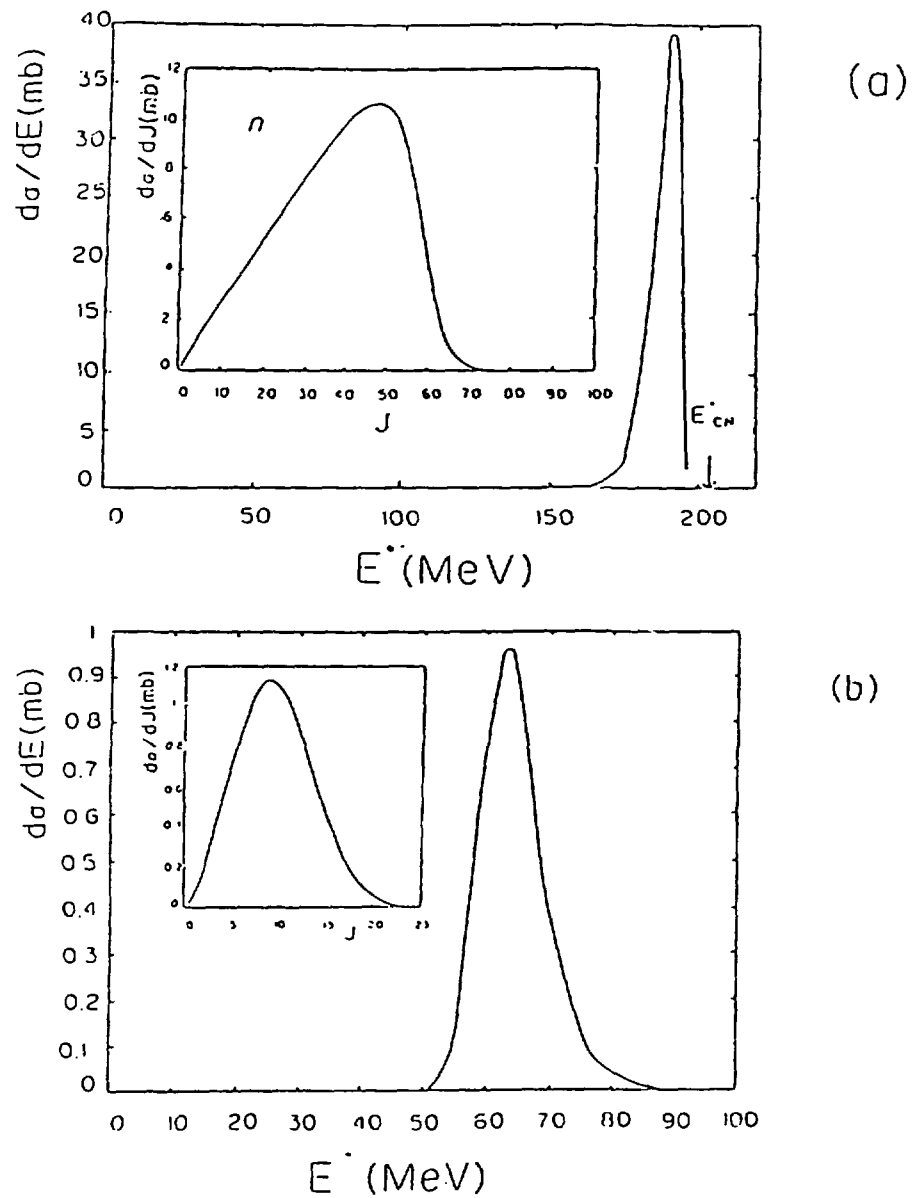


Fig.7 Excitation energy distributions of the residue nuclei of light particle emissions and fission fragment obtained by the first step EIF-method calculation for the $^{84}\text{Kr} + ^{27}\text{Al}$ reaction at $E_{\text{Lab}} = 890\text{MeV}$. The inset are the spin distribution of the first chance emission and fission fragment. (a) neutron emission, (b) fission fragment of $Z = 23, N = 29$.

and higher excitation energy around $E^* \approx 30\text{ MeV}$, these light fragments also decay by emitting the light particles. Therefore, these residue nuclei started from the produced

light fragments at first step shift down to the nuclei with smaller charge. This may be one of the possible interpretation of the complex fragments production.

Effect of the multi step EHF-calculation.

Next the results of the final step obtained by the full cascade calculation are shown. In Fig.8 the calculated charge distributions are shown by comparing the measured one [2].

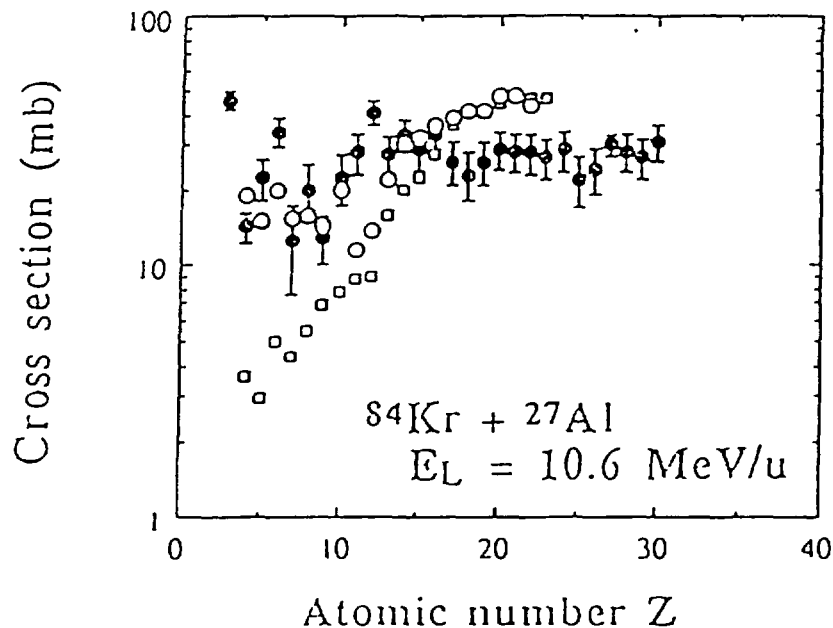


Fig.8 Comparison of the measured Z-distribution (closed circles) [2] and calculated Z-distribution obtained by EHF-method calculation for the $^{84}\text{Kr} + ^{27}\text{Al}$ reaction at $E_{Lab} = 890\text{MeV}$. The open squares show the results of first-step calculation and open circles the results of multi-step cascade calculation.

The large enhancements from the first step distribution in the region of light fragments $Z < 10$ are obtained. The main origin of the enhancement around $Z \simeq 10$ is the light particle cascade decay of fission-like fragments with a few larger mass. On the other hand the enhancements in the region $Z < 7$ come from the multi-step cascade decay of the evaporation residues in the first step. Because the calculated charge distribution in the region of symmetric fission is somewhat larger than the measured one, the values of the calculated cross sections in the lighter fragments become somewhat small by comparing the measured ones.

In Fig.9(a) and (b), the calculated isotope mass distributions for the case of Si and Ca isotope are shown comparing with the observed ones, respectively. As can be seen in the observed isotope mass distributions (see Fig.11 of Ref.[2]), the distribution of each isotope has the peak around the nucleus of the beta-stable-line. The peak of the calculated distributions obtained in the first step EHF-calculation deviates to the heavier part by two or three mass units than the observed one. However, as we have already discussed on the spin and energy distribution of fission-like fragment at first-

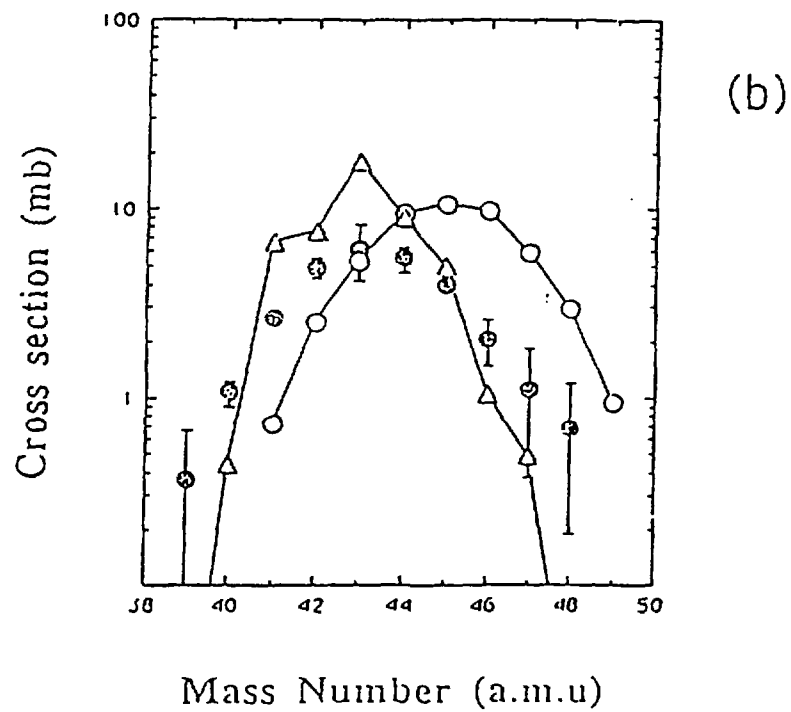
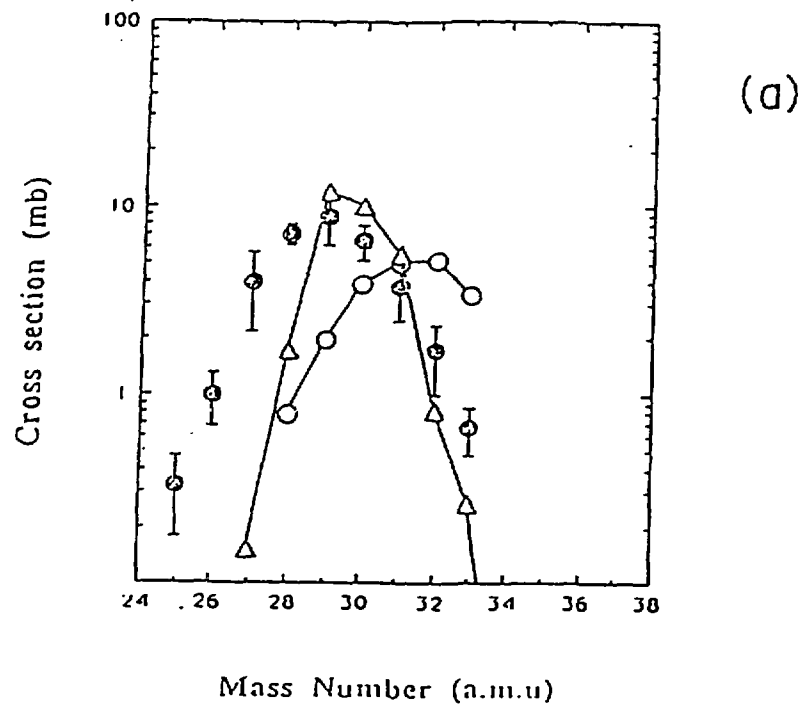


Fig.9 Comparison of the measured isotope mass-distribution (closed circles) [2] and calculated distribution obtained by EIF-method calculation for the $^{84}\text{Kr} + ^{27}\text{Al}$ reaction at $E_{\text{Lab}} = 890\text{MeV}$. The open circles show the results of first-step calculation and open triangles the results of multi-step cascade calculation. (a) shows Si isotope (b) Ca isotope.

step calculation shown in Fig.7(b), the fragments decay by emitting the particle. Then as a consequence of the multi-step cascade decay, the peak of the distribution of the first-step shifts down and the calculated distribution of the final-step reproduces well the observed one.

Finally the calculated kinetic energy distributions for the $Z = 20$ fragment is shown in Fig.10 by comparing with the measured one. The kinetic energy distribution is calculated by taking into account the effect of multi-step cascade decay of fission-like fragments. At first the kinetic energy distribution in the CM-system are transformed to the laboratory system with the laboratory angle θ_L by assuming that the angular distribution of decaying fragment in the CM-system has the $1/\sin(\theta)$ dependence. Next it is assumed that the velocities of the fragments conserve in the process of the light particle cascade decay. Then the kinetic energy distribution are evaluated as shown in Fig.10. By comparing with the thus calculated and the measured kinetic energy distributions, the calculated results reproduce well the observed one except that the width of the calculated one is somewhat narrower than the measured one.

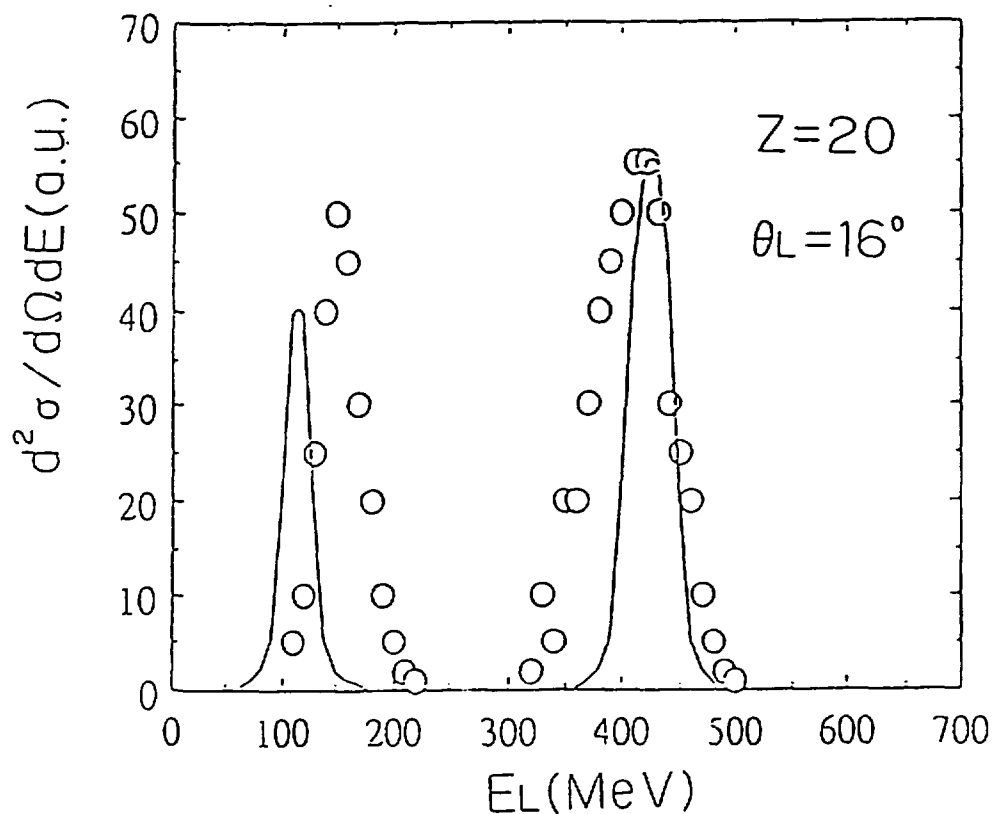


Fig.10 Comparison of the measured kinetic energy distribution (open circles) [2] and calculated distribution (solid line) obtained by EHF-method calculation for the $^{84}\text{Kr} + ^{27}\text{Al}$ reaction at $E_{Lab} = 890\text{MeV}$ at $\theta_L = 16^\circ$. The calculated kinetic energy distribution is for the fragments with $Z = 20$ at final step after the sequential multi-step cascade calculation from all available fragments.

5. Conclusions.

It is shown that the observed quantities of the complex fragment productions (fission-like productions) and the evaporation residues are well reproduced by the *EHF-method* for both $^{35}\text{Cl} + ^{12}\text{C}$ and $^{23}\text{Na} + ^{24}\text{Mg}$ reactions. The essential point of the *EHF-method* is to treat the light-particle emission and heavy fragment production in equivalent statistical way and practically to utilize fully the effect of the observed binding energy in the calculation. Then it is expected that the decaying compound nucleus has to be represented by a statistical ensemble of the binary combination of almost individual nuclei. It is very important that the significantly large amount of cross section of the fission-like fragment production really exist as a part of complete fusion cross section in the lighter mass system. Then in order to make clear which theoretical model is valid, it is hoped that the experimental studies on the complex fragment production will be performed more systematically at higher energy region in the lighter mass system.

On the complex fragment production from the ^{111}In compound nucleus formed by the reaction $^{84}\text{Kr} + ^{27}\text{Al}$ at $E_{\text{Lab}} = 890\text{MeV}$, the *EHF-method* was also applied and the processes of the multi-step cascade decay of the fission-like fragments and the evaporation residues are investigated by referring the statistical binary decay of the ^{47}V compound nucleus. It was shown that the significant enhancement from the first step calculation of the intermediate mass production such as $Z < 10$ comes from not only the sequential multi-step cascade decay of the fission-like production but also the evaporation residues. The isotope mass distributions which will give the essential criterion for the study on the reaction mechanism are well reproduced by the *EHF-method* including the sequential multi-step cascade decay of the fission-like production.

ACKNOWLEDGMENTS

One of us(T.M.) would like to acknowledge Mr. T.Takizawa for his kind assistance. The whole calculations of this study are performed by the use of computers H260D of Shinshu University, M880 of University of Tokyo and F780 of RIKEN.

REFERENCES.

- [1] B.Heusch, contribution to this conference.
- [2] K.Yuasa-Nakagawa et al., contribution to this conference, and references therein.
- [3] G.Guillaume, et al., Phys. Rev., C26(1982) 2458.
- [4] J.P.Coffin, et al., Phys. Rev., C30 (1984) 539.
- [5] S.J.Sanders, et al., Phys. Rev., C40 (1989) 2091.
- [6] L.G.Moretto, Nucl. Phys., A247 (1975) 211.
- [7] B.Shivakumar, et at., Phys. Rev., C35 (1987) 1730.
- [8] C.Beck, et al., Z. Phys. A334 (1989) 521.
- [9] C.Beck,et al., Proc. of the Workshop on the Interface between Nuclear Structure and Heavy-Ion Reaction Dynamics, Notre Dame, May, 1990; Inst. Phys. Conf. Ser. n° 109 (1990) 213.
- [10] T.Matsuse, Proc. of the Tsukuba Intern. Symp. on Heavy Ion Fusion Reactions, edited by K.Furunc and T.Kishimoto (Tsukuba,Japan,1984) 113.
- [11] S.M.Lee, W.Yokota and T.Matsuse, Proc. of the Symp. on the Many Factes of Heavy Ion

- Fusion Reactions, (Argonne 1986) 63.
- [12] T.Matsuse, Proc. of International Symposium on Heavy Ion Physics and Its Application, Lanzhou, China, Oct 1990, edited by W.Q.Shen, Y.X.Luo and J.Y.Liu (World Scientific) 95, and references therein.
 - [13] B.Djerroud et al., Proc., of 6th Intern. Conf. on Nuclear Reaction Mechanisms, Varenna, 10-15 June 1991.
 - [14] S.M.Lee et al., Nucl. Phys. A519 (1990) 221c. and Proc. of International Symposium on Heavy Ion Physics and Its Application, Lanzhou, China, Oct 1990, edited by W.Q.Shen, Y.X.Luo and J.Y.Liu (World Scientific) 401.
 - [15] S.M.Lee, T.Nakagawa and T.Matsuse, Proc. of the Tsukuba Intern. Symp. (1984),p.62.
 - [16] A.Bohr and B.R.Mottelson, "Nuclear Structure Vol.1"
 - [17] A.H.Wapstra and G.Audi, Nucl. Phys., A432(1985) 1.
 - [18] H.J. Krappe and J.R. Nix, Proc. of the Third Int. I.E.A. Symp. on the Physics and Chemistry of Fission,(Vinna 1973),Vol.1,p.159